ChemComm

FEATURE ARTICLE

View Article Online
View Journal | View Issue

Cite this: *Chem. Commun.*, 2025, **61**, 4774

Functional design of metal aerogels for wearable electrochemical biosensing devices

Pengxin Xue,[ac] Shaokun Zhou,[b] Guanglei Li *[ac] and Dan Wen *[b]

Received 25th December 2024,
Accepted 20th February 2025

DOI: 10.1039/d4cc06728b

rsc.li/chemcomm

Metal aerogels (MAs) represent a novel class of aerogels composed entirely of interconnected metal nanoparticles or nanostructures. They integrate the unique physicochemical properties of metals with the high surface area and porosity of traditional aerogels, resulting in high electrochemical activity, efficient mass and electron transport, and considerable mechanical stability. These attributes make MAs particularly appealing for applications in wearable electrochemical biosensing devices. As electrode materials for electrochemical sensors, MAs can serve as carriers for enzymes or as electrocatalysts (with inherent electrocatalytic properties), thereby delivering superior sensing performance. Moreover, their three-dimensional, interconnected network structure imparts inherent flexibility, making them highly suitable for wearable biosensor electrodes. This review highlights recent advancements in the functional design of MAs for wearable electrochemical sensors and evaluates their performance in human biomarker monitoring. It also explores the challenges and future potential of MAs in such wearable devices. With ongoing progress in materials science, MA-based wearable biosensors hold significant promise for advancing disease diagnosis and health management.

Introduction

Recent advances in health monitoring tools have fueled growing interest in the rapid and reliable *in situ* analysis of biological samples for disease diagnosis and health management.[1,2] Various biological matrices, including blood, interstitial fluid (ISF), saliva, tears, and sweat, are replete with biomarkers indicative of physiological and health status, making them ideal for *in situ* chemical analysis.[3] Electrochemical assays, known for their high sensitivity, excellent selectivity, and rapid response, offer distinct advantages in medical and healthcare applications.[4–7] Since the introduction of the amperometric glucoamylase electrode by Clark in 1962, electrochemical-based assays have witnessed remarkable progress.[8–12] Despite these advancements, biosensor performance is often validated only in artificial rather than clinical samples.[13] To expand the scope of these assays and enable real-time monitoring, utilizing the inherent miniaturization and low-power consumption characteristics of electrochemical sensors and integrating them into portable, wearable or implantable devices can not only facilitate faster, more convenient prompt on-the-spot testing (POCT), but also significantly shorten the diagnostic cycle, bringing innovations in the medical field.[14–18]

Currently, wearable electrochemical biosensors typically consist of a support substrate, a sensing element, and a signal output unit.[19] For these sensors to be effective, they must exhibit robust sensing performance and maintain efficient, stable operation even under significant deformations, such as bending, stretching, or twisting.[20,21] Traditional wearable sensors often rely on rigid nanomaterials which are mounted on inflexible substrates, like conductive glass. This rigid configuration limits their ability to integrate seamlessly with soft human skin or clothing, restricting their practical applications. Thus, researchers developed sensors based on flexible substrates such as conductive polymer films and conductive hydrogels.[22–25] However, the sensitivity, which is the key parameter of the sensors, could not be maintained very well after the deformations due to the unstable catalytic properties of the sensing materials. Therefore, exploring sensing materials with high catalytic activity as well as unique flexibility is of great significance for advancing wearable electrochemical sensing technology.

Metal aerogels (MAs) are a new class of porous materials constructed entirely from nanostructured metals. Their unique porous structure, high specific surface area, excellent electrical conductivity, and superior catalytic activity make them highly versatile, with a wide range of applications across various fields.[26–29] Notably, MAs offer significant advantages in wearable electrochemical biosensing devices: (1) the hierarchical porous structure and high specific surface area facilitate the dispersion and immobilization of enzymes, enhance selectivity,

[a] *Interdisciplinary Research Center of Biology & Catalysis, School of Life Sciences, Northwestern Polytechnical University, Xi'an 710072, China. E-mail: lgl_ldf@nwpu.edu.cn*
[b] *State Key Laboratory of Solidification Processing, School of Materials Science and Engineering, Northwestern Polytechnical University, Xi'an 710072, China. E-mail: dan.wen@nwpu.edu.cn*
[c] *State Key Laboratory of Transducer Technology, Shanghai Institute of Microsystem and Information Technology, Shanghai 200050, China*

and simultaneously accelerate mass transfer to improve sensitivity during electrochemical biosensing. (2) The conductive metal skeleton can promote efficient electron transfer in the bio-/electrocatalytic reaction, further enhancing sensitivity. (3) MAs can directly catalyze target molecules, eliminating the need for the harsh reaction conditions required by enzyme-based sensors, thus improving stability and offering potential as enzyme substitutes. (4) The interconnected nanowire structures of MAs ensure consistent functionality of sensing electrodes under mechanical deformations such as expansion, contraction and folding, providing flexibility and reliability for wearable applications. These characteristics make MAs ideal flexible electrochemical sensing materials for the development of wearable devices and flexible electronics with significant potential in biomedical and health monitoring.

In this review, we summarize recent advances in the field of wearable electrochemical biosensing devices using MAs, as illustrated in Fig. 1. We begin by discussing the preparation and functionalization strategies together with the key properties of MAs, highlighting their key properties and versatility in *in vitro* biosensing applications. We then focus on the recent developments in wearable electrochemical biosensing devices based on MAs, showcasing their excellent performance and potential for practical applications, such as monitoring organic compounds and ions in body fluids. An overview of the strategies employed to achieve wearability in these devices is also presented. Finally, we address current challenges and outline future trends for the application of MAs in wearable biosensing devices.

Metal aerogels

In 2008, Qin *et al.* firstly discovered that, by simply adjusting the pH, Au nanoparticle sols could be induced to form self-supported aggregates, which were further dried to produce Au sponges.[30] Then the concept of MAs was formally proposed in the following year, with related research initiated by the Eychmüller group, who synthesized a series of macroscopic, self-supported MAs.[31] Since then, nearly a decade of intensive development has resulted in significant progress in both the synthesis and application of MAs. A variety of MAs with highly porous nanostructures have been reported, ranging in composition from single metals (Au, Ag, Pd, Pt) to multiple alloys (Au–Pd, Pd–Pt, Au–Pd–Pt, Cu–Ir),[32–35] and in microstructure nanowires or nanochains to nanosheets.

Preparation and functionalization

Efficient synthesis strategies are fundamental in determining the structure and function of materials as well as the range of applications. There are many methods for preparing metal foams with a reticulated porous structure similar to that of aerogels, including non-sol–gel methods,[36–39] such as dealloying, template methods, high-temperature reduction, combustion synthesis, and direct freeze-drying methods. For the preparation of MAs, sol–gel methods are usually employed. The wet gel is first prepared in a solution phase, followed by freeze-drying or supercritical drying to obtain aerogels. The sol–gel method has been one of the most promising methods for the preparation of metal aerogels due to its mild reaction conditions, simple preparation process, excellent composition, and strong structural control. There are two typical generic pathways for the preparation of metal aerogels by the sol–gel method (Fig. 2).

Strategy I: two-step method. The advantage of the two-step synthesis strategy for preformed metal NPs is that the formation and assembly of NPs are two relatively independent processes, which facilitates fine tuning and mechanistic studies.

Firstly, metal nanoparticle sols can be obtained by reducing metal precursors, in which the stabilisers are ionised or hydrolysed to form metal NPs with ligands attached to their surfaces,

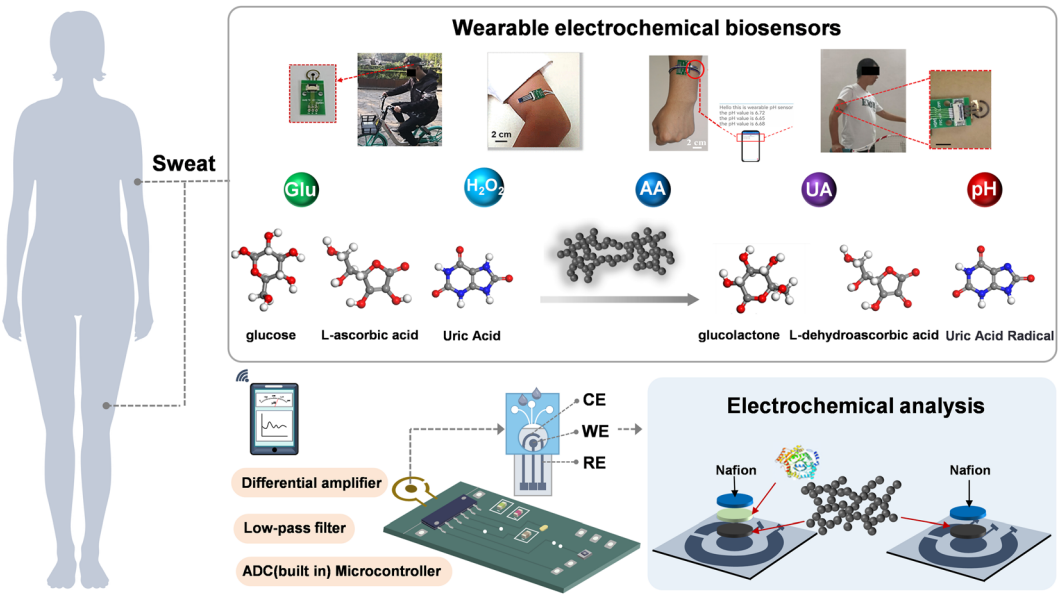

Fig. 1 Electrochemical wearable biosensors based on MAs.

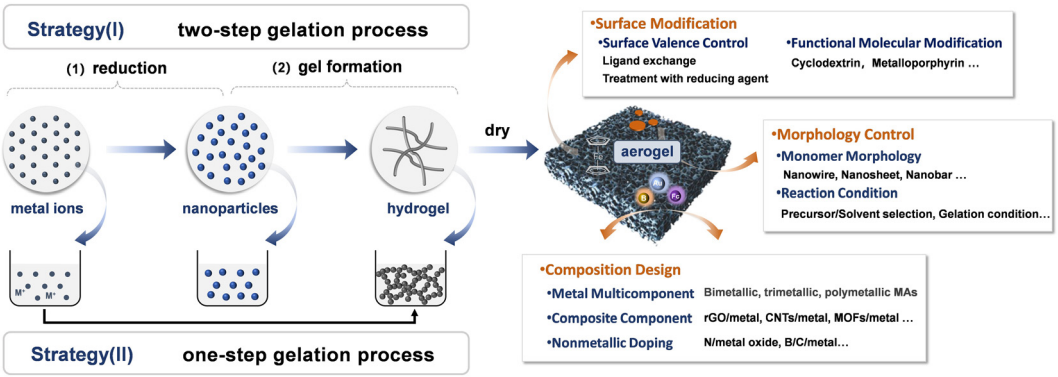

Fig. 2 Preparation and functionalization strategies of MAs.

inducing electrostatic repulsion and spatial site-disturbance effects to balance the van der Waals forces between the NPs and thus ensure colloidal stability. Subsequently, impurities and excess stabilisers are removed by filtration and concentration, and oxidants or undesirable solvents are used as initiators to induce gelation. As the NPs are connected, the sol is gradually destabilised and finally hydrogels form and settle to the bottom of the container. MAs are obtained by removing the solvent from the wet gel without changing the network structure.[40,41] Unlike the conventional strategies of carbothermal reduction of metal oxides and introduction of linkers,[42,43] pure MAs with fine structures can be prepared using the sol–gel two-step method, and the post-treatment process does not require a high-temperature sintering step. However, the current one-step preparation of aerogels has received a lot of attention due to the more straightforward and simpler synthesis steps.

Strategy II: one-step method. For the one-step reduction synthesis strategy of *in situ* spontaneous gelation, Liu *et al.* were the first to prepare Pd aerogels using $NaBH_4$ as a reducing agent, thus pioneering the one-step reduction approach of the sol–gel method.[44] Although the gelation mechanism is still unclear, this work provided a new idea for the subsequent facile preparation of MAs, and many MAs based on Au, Pt, Ag, Cu, and Ni were successively developed.[45] Accelerated gelation can be achieved by controlling the temperature and adjusting the reducing agent. Jin *et al.* successfully reduced the preparation time of PtRh alloy gels to 5–8 h by adding $NaBH_4$ to H_2PtCl_6–$6H_2O$ and $RhCl_3$–$3H_2O$ solutions.[46] $NaBH_4$ is the most commonly used reducing agent for the one-step preparation of MAs, while N_2H_4–H_2O, ascorbic acid (AA), dimethylamine borane (DMAB), and NaH_2PO_2 are also applied in small amounts. The formation and development of the 3D structure of MAs can be altered by designing and regulating the conditions such as the type of reductant and the amount of dosing, and the external physical field, which can then determine their final catalytic performance. Jiang *et al.* chose a strong reducing agent, $NaBH_4$, a moderate reducing agent, DMAB, and a weak reducing agent, AA, for the reduction of $Ni(AC)_2$, $Cu(AC)_2$, and $Fe(AC)_2$ solutions, respectively, for the preparation of MAs.[47] The results showed that only DMAB was able to induce the generation of aerogels constructed by Cu@Fe@Ni NPs with a core–shell structure, which was based on the principle that the difference in the reducing potential of the metal ions induces the difference in the rate of the nanoparticle formation. Compared with the two-step method, the one-step synthesis strategy offers significant advantages in adjusting the proportion and composition of materials, but it has limitations in controlling the microstructure of aerogels.

Additionally, by functionalizing the morphology, composition and surface properties of MAs, their electrochemical activity can be significantly improved, laying the foundation for the construction of high-performance wearable electrochemical sensors. Fang *et al.* modulated the electronic structure of Au aerogels by doping very low levels of Bi as a synergistic component into Au aerogels.[48] A large number of holes were generated on the surface of the optimised AuBi aerogels, which were able to oxidise OH^- to $^{\bullet}OH$ and thus oxidise glucose at a faster rate. Cai *et al.* prepared hierarchical porous aerogels with well-defined 3D network structures using PdNi hollow nanospheres (HNSs) as nanobuilding units (NBBs), which exhibited higher electrocatalytic activity in ethanol oxidation reactions.[49] Alternatively, modification of MAs by using partially reduced graphene oxide (rGO) or conductive polymers (*e.g.*, polypyrrole, polyaniline) can also be used to improve mass transport within the gels and their electrical conductivity, thereby facilitating the penetration of electrolytes and biomarkers. Yuan *et al.* employed metal porphyrins (FeTPyP) as a crosslinking agent to facilitate the 3D assembly of metal NPs (such as Pt, Pd, Au, Ag and Pt–Pd NPs) into molecular-metal aerogels (M-NMAs), which demonstrated significantly enhanced ORR activity and durability in different electrolytes.[50] Thus, the functional design of MAs enhances their electrochemical activity and imparts unique properties, significantly expanding their potential applications in wearable electrochemical sensing. The following section will provide a detailed discussion on how these modifications contribute to improved performance in wearable electrochemical biosensing applications.

Properties

This section highlights the key characteristics of MAs, including their mechanical properties, electrical conductivity, and processability, which together underscore their potential in wearable electrochemical biosensing. The most critical function, electrochemical

activity, will be discussed in detail in the next section, along with their biosensing application.

Mechanical properties. MAs prepared *via* the sol–gel method often exhibit poor mechanical properties, such as low fracture toughness and tensile strength, due to stress concentration, small feature sizes, and incomplete gel network development caused by microstructural inhomogeneity. However, certain aerogels demonstrate good elastic and mechanical properties, attributed to the high aspect ratio of their highly branched nanowire structures. In recent years, researchers have enhanced the mechanical strength of MAs by adjusting alloy compositions, optimizing preparation strategies, and refining synthesis processes.

Pan *et al.* prepared highly compressible and air-dryable Ni nanowire aerogels (NNWAs) by a magnetic field-assisted gelation strategy.[51] As shown in Fig. 3a, the unique anisotropic lamellar structure and abundant cold-welded junctions of intertwined nanowires endow NNWAs with excellent electrical conductivity and compression fatigue resistance, like a maximum strain of 70% and high compression fatigue resistance, maintaining over 90% height retention after 500 loading–unloading cycles. Xu *et al.* synthesized Cu NW aerogels with adjustable density by regulating the bubble concentration change during the preparation process through the reduction of $CuSO_4$ solution with N_2H_4–H_2O as the reductant and ultrasonic treatment (Fig. 3b).[52] The Cu NW aerogels can recover to the original height after a 60% strain loading–unloading cycle and show good mechanical compliance. When used as sensitive electrode materials for pressure sensors, they respond rapidly (within 80 ms) and exhibit excellent fatigue resistance.

Electrical conductivity. Due to their high electrical conductivity, MAs are considered promising materials for electronic sensing devices. Several studies have focused on enhancing the electrical conductivity of MAs by optimizing their composition, such as incorporating highly conductive metals like Cu, Ag and Au to facilitate electron transport or modulate the electrical conductivity. Tang *et al.* synthesized Cu NWs aerogels by reducing $Cu(NO_3)_2$ using N_2H_4–H_2O and freeze-drying.[53] By adjusting the density of the aerogels (15.55–4.6 mg cm^{-3}), they effectively controlled porosity, minimized defects, and optimized nanowire connections, achieving systematic tuning of the conductivity (90–176 S m^{-1}). Given its superior electrical conductivity and chemical stability compared to Cu, Ag is being actively investigated for the preparation of high-performance conductive aerogels. Jung *et al.* firstly reported the preparation of Ag NW aerogels by assembling Ag NWs from their colloidal suspensions into crosslinked networks in the transition from dilute to isotropic concentrated states.[54] Qian *et al.* prepared Ag NWs using a modified polyol synthesis method.[55] By controlling the density of the aerogels, they achieved tunable electrical conductivity and structural strength, with a maximum conductivity of 51 000 S m^{-1}.

Processability and integrability. Effective integration of 3D porous and irregularly shaped MAs into sensing devices is critical for practical applications. Although this process is still challenging, many options have been developed to improve the processability of MAs. Through impregnation, evaporation of solvents, inkjet printing, electrostatic spinning, and other micro-nanofabrication techniques, deposition or printing of MAs on flexible substrates not only simplifies the process, but also improves the homogeneity and controllability of materials. Meanwhile, by introducing surfactants or other modifiers, the surface properties of MAs can be improved to enhance their conductive stability and mechanical properties over a wide range of strains. For example, Lübkemann *et al.* obtained porous 3D CdSe/CdS gel network coated films by simultaneously printing CdSe/CdS nanorods and a destabilising agent (H_2O_2) on conductive tin-doped indium oxide coated glass surfaces using inkjet printing technology (GelVIP). The precise deposition of such nanoparticle-based gel-coated films not only enhances the movement/diffusion of charge carriers in the gel structure, but also contributes to the preparation of small-area patterned electrodes for flexible electronic device applications.[56] Fig. 4a shows the SEM image of the MA film deposited on the glass substrate.

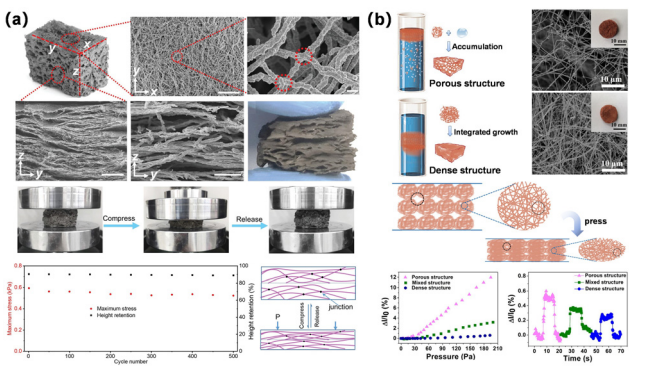

Fig. 3 (a) Morphology and mechanical properties of NNWAs (copyright 2022, John Wiley and Sons).[51] (b) Controlled fabrication of Cu NW aerogels with different structures and pressure-response for aerogels (copyright 2017, American Chemical Society).[52]

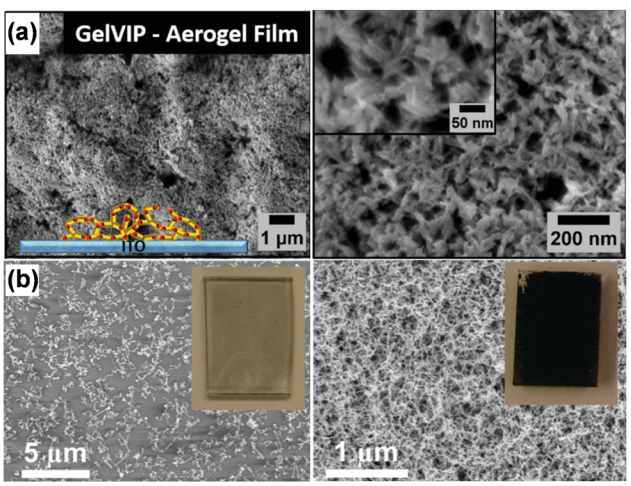

Fig. 4 (a) Schematic illustration and SEM images of a highly porous printed CdSe/CdS nanorod-based aerogel network on conducting ITO substrate by GelVIP technology (copyright 2012, American Chemical Society).[56] (b) SEM images of a thin Au network (left) and Au/Ag (right) aerogel films formed on a glass substrate with the aid of poly(diallyl dimethylammonium chloride) (copyright 2019, John Wiley and Sons).[57]

Another way to improve processability is to prepare gel–polymer composites. Gel–polymer composites can be prepared by infiltrating a monomer solution into the pores of MAs and initiating a polymerization reaction inside, which not only have good mechanical strength, but also maintain the high porosity and conductivity of the aerogels. As shown in Fig. 4b, the Eychmüller group used ethyl cyanoacrylate as the monomer, infiltrated it into Au–Ag–Pt aerogels and cured it, and the microscopic morphology of the formed composites showed a uniform and completely filled pore structure, which can be further processed into desired geometries by cutting and shaping.[57] The improved processability of the MAs not only enhances the mechanical and handling properties of the aerogels, but also retains their unique physicochemical properties, which offers the possibility of integration in wearable biosensing applications.

Wearable electrochemical biosensors based on MAs

With breakthroughs in sensor technologies, electrochemical sensors are being further miniaturized and integrated into wearable accessories and clothing for personal biomonitoring and personal microenvironment monitoring.[58–62] Considering that modifying sensing electrode nanomaterials can enhance the sensitivity and selectivity of electrochemical sensors,[63] addressing the challenges in developing electrochemical wearable biosensing devices requires continued research into advanced electrode materials to meet the practical demands of future healthcare applications. Electrochemical biosensing based on MAs shows great potential for *in situ*, real-time monitoring due to their high electrical conductivity and catalytic activity as well as good mechanical properties. Porous MAs with a 3D structure and high surface area can be utilized as immobilized enzyme carriers for electrochemical biosensing, while their high electrocatalytic activity enables the direct detection of biomarkers.[64] Notably, the 3D networks of highly branched, interconnected nanowires endow MAs with unique physical properties, such as intrinsic flexibility and self-healing capabilities, which have been successfully applied in the development of flexible electrodes for wearable biosensing applications.

MA-based electrochemical biosensing platform

Enzymes are widely used in biosensors as efficient biorecognition elements that selectively react with biomarkers and generate specific signals. To enhance their stability and prevent shedding, enzymes require robust carriers for dispersion and immobilization. Porous materials with a 3D structure and high surface area are ideal for this purpose.[65–67] MAs offer significant advantages for enzyme immobilization due to their unique physicochemical properties. The high specific surface area of MAs enables greater enzyme adsorption and immobilization, increasing enzyme loading, catalytic efficiency, and the sensing signal. Additionally, the high porosity and 3D self-supporting structure of MAs facilitate electrolyte and biomarker penetration, while providing abundant reaction sites that preserve enzyme activity and enhance catalytic reactions. Therefore, enzyme-loaded MAs also promote efficient electron and mass transfer through their porous structure, delivering intrinsic catalytic activity and fast, reversible electron transfer kinetics. These features make them highly promising for improving the sensitivity, selectivity, and stability of bioelectronic devices. For instance, Wen *et al.* developed a facile method with calcium ions as the destabilizing agent to prepare Pd aerogels, achieving high glucose bioelectrooxidation activity when co-immobilized with glucose oxidase (Fig. 5(a1)).[68] The resulting enzyme electrode demonstrated a sensitivity of 1.11 μA mM^{-1} in the 2–20 mM glucose range, which is 125 and 3 times higher than those of GC and Pd NPs as enzyme supports, respectively. This superior performance is attributed to the porous structure of aerogels, which not only allow fast transport of the substrate as

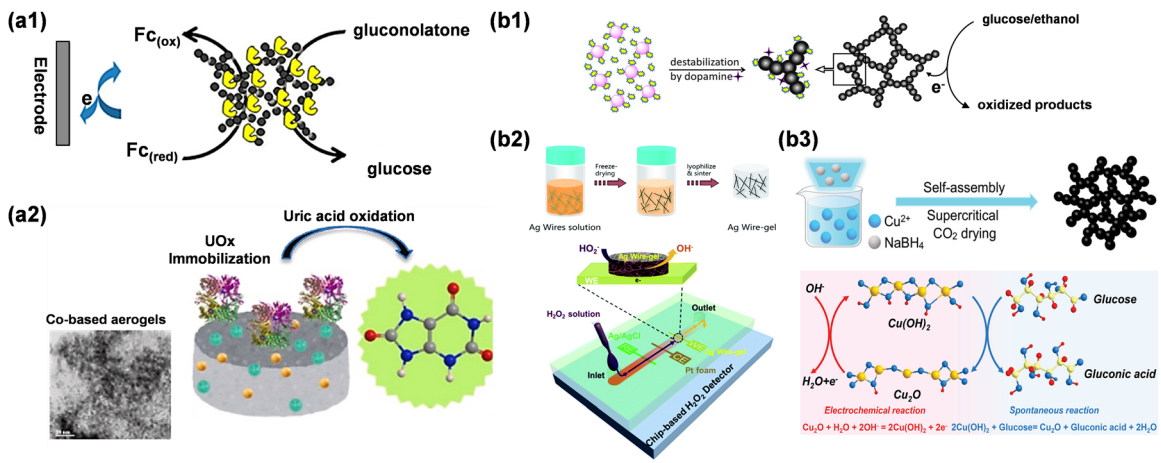

Fig. 5 An electrochemical biosensing platform for biological/non-biological enzymes based on MAs. (a1) Pd aerogels co-immobilized with GOx (copyright 2014, American Chemical Society).[68] (a2) Co-based aerogels co-immobilized with UOx (copyright 2025, Elsevier).[69] (b1) Preparation strategy of an Au-based nonenzymatic glucose sensor (copyright 2016, American Chemical Society).[70] (b2) Preparation strategy of an Ag-based nonenzymatic H_2O_2 sensor (copyright 2019, Royal Society of Chemistry).[71] (b3) Preparation strategy of a Cu-based nonenzymatic glucose sensor (copyright 2023, John Wiley and Sons).[72]

well as the mediator through the electrolyte/electrode interface due to a short diffusion length but also ensure contact with a larger surface due to the high surface area. Furthermore, Pd aerogels enhanced the conductance within the enzyme film and improved the electrical communication between the electrode and the ferrocene units that mediate the bioelectrocatalytic oxidation. Similarly, as shown in Fig. 5(a2), Ruiz-Guerrero *et al.* prepared Co-based aerogels conjugated with uric acid oxidase (UOx) for bioelectrocatalytic uric acid (UA) detection.[69] Co-based aerogels showed a decrease in overpotential and an increase in current density in the presence of UA, which was attributed to the inherent electrochemical activity of materials themselves as well as the high surface area providing more active sites. These studies highlight the immense potential of enzyme-immobilized MAs for developing electrochemical biosensors capable of reliable application in biological fluids.

Metal aerogels (MAs), known for their high electrocatalytic activity, have been widely explored for the direct detection of biomarkers such as glucose, H_2O_2, uric acid (UA), and ascorbic acid (AA), which are integral to numerous physiological and pathological processes.[73–75] As shown in Fig. 5(b), MAs derived from highly conductive noble metals like Ag and Au facilitate efficient electron transport and exhibit superior electrocatalytic activity. Wen *et al.* reported a facile and versatile strategy for the formation of an Au aerogel involving the dopamine-induced 3D assembly of Au nanoparticles.[70] The prepared Au aerogel exhibited high activity toward glucose oxidation with a sensitivity of 332.9 $\pm$ 7.6 $\mu A\ mM^{-1}\ cm^{-2}$. Yang *et al.* demonstrated an application example of using Ag aerogels for microfluidic H_2O_2 biosensing chips.[71] The high porosity and hierarchical porous structure of Ag NW aerogels with nanowires of 250 nm diameter, uniformly covered with the organic ligand polyvinylpyrrolidone, effectively avoid the oxidation of Ag and the generation of contact resistance. These Ag NW aerogels exhibited higher electrocatalytic activity and cycling stability compared to commercial Ag rods and Ag NWs loaded on carbon cloth. Alternatively, non-noble metal-based MAs offer cost-effective alternatives with similarly excellent sensing performance. Fang *et al.* developed single-component Cu aerogels and explored the structure–activity relationship between non-enzymatic glucose sensing and its catalytic mechanism using a sustainable Cu(I)/Cu(II) redox cycle.[72] Due to the unique structure of aerogels, Cu aerogels showed excellent performance in electrocatalytic oxidation of glucose, achieving the non-enzymatic glucose sensing target with a low detection limit (0.48 μM) and high sensitivity (414.3 $\mu A\ mM^{-1}\ cm^{-2}$).

Clearly, MA-based electrochemical biosensing platforms \demonstrate excellent sensing performance, both in facilitating the biological recognition of target molecules when enzymes are immobilized and in directly responding to target molecules as electrocatalysts. Coupled with the excellent mechanical properties of MAs, these platforms show tremendous potential in the field of wearable electrochemical biosensors. Despite significant progress in electrochemical biosensing with MAs, many electrochemical sensors have not yet been widely used in real-world scenarios due to technical limitations (*i.e.*, reliability, durability, selectivity, and the integration process).[76,77] Consequently, researchers are actively exploring the transition pathways from lab-scale electrochemical biosensing platforms to practical wearable electrochemical sensors. Advances in microfabrication and nano-engineering have generated considerable research interest, with technologies such as screen printing (SPE) and microelectromechanical systems (MEMS) enabling the development of smaller and more integrated wearable devices.[78,79] In addition, the incorporation of machine learning algorithms and intelligent data analytics facilitates the effective processing and interpretation of sensor data, providing users with real-time, accurate health monitoring information.[80,81] Therefore, with continued technological advances, wearable electrochemical sensors based on MAs are poised to play a pivotal role in health monitoring, disease diagnosis, and related fields, advancing personalized medicine and offering more convenient and intelligent services.

MA-based wearable electrochemical biosensing

Miniaturization and integration are key trends in electrochemical biosensors, particularly for wearable devices that enable dynamic real-time monitoring of biomarkers *in vivo*.[82] To date, small molecules like glucose, UA, AA, and H_2O_2 in body fluids have been extensively studied using wearable electrochemical sensors, and conventional sensing electrodes are typically noble metal thin films (Au, Pt).[83] Recent advances in materials science have introduced MAs as promising electrode materials due to their exceptional electrochemical activity, excellent mechanical properties as well as ease of integration. These attributes have significantly enhanced the performance of wearable sensors. Our research group has been at the forefront of developing wearable electrochemical biosensors based on MAs, achieving notable progress in biomarker monitoring through sweat – a commonly analyzed body fluid rich in diverse targets.

Abnormal metabolism of glucose is a major contributor to diabetes, pancreatitis and other complications. Non-invasive and real-time monitoring of biomarkers is crucial for improving the health and quality of life for patients. Li *et al.* reported wearable electrochemical biosensors that integrated highly porous and flexible Au hydrogels with soft-MEMS technologies, where a redox enzyme was immobilized on an Au hydrogel to fabricate biosensing chips.[84] As illustrated in Fig. 6, hierarchical porous Au hydrogels were developed through dopamine-induced self-assembly of Au NPs, which can flow and float on the water surface and fold into different shapes with great flexibility. Additionally, Au gels demonstrated excellent electrocatalytic activity towards H_2O_2, a byproduct of many oxidases, enabling the quantitative determination of corresponding targets by measuring the amount of H_2O_2 produced during the reaction with small molecules. Given the significance of glucose monitoring, GOD was initially chosen as a model enzyme for the Au aerogel-based sensing electrode. The biosensor exhibited high sensitivity (10.51 $\mu A\ mM^{-1}\ cm^{-2}$), stability for over 15 days, and good selectivity. It also maintained almost constant performance under mechanical deformation (0–90°) with minimal deviation of less than 1.84%. Furthermore, when lactate oxidase was incorporated into the Au hydrogels, the wearable biosensing

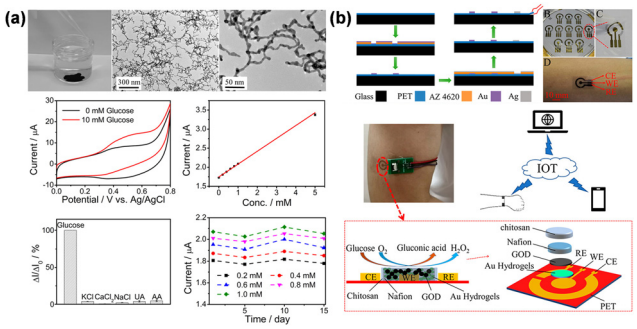

Fig. 6 Integrating highly porous and flexible Au aerogels with soft-MEMS technologies for high-performance wearable biosensing.[84] (a) The optical image, micromorphology and electrochemical test results of Au aerogels. (b) Manufacturing processes of MEMS electrodes (copyright 2021, American Chemical Society).

platform exhibited broad applicability, effectively detecting various biomarkers such as lactate in sweat. This pioneering study is the first to employ MAs in wearable biosensing devices, showcasing their feasibility and versatility.

Enzymatic electrodes are known for their good selectivity, making them important in wearable glucose sensing. However, non-enzymatic electrodes have garnered more attention due to the instability of enzyme activity, which can compromise long-term sensor performance. Li *et al.* demonstrated a strategy that combines compositional and structural engineering to design PtNi dual-structured aerogels for non-enzymatic wearable glucose sensing monitoring in sweat.[85] As shown in Fig. 7a, the 3D PtNi MAs featured interconnected networks of PtNi nanowires and $Ni(OH)_2$ nanosheets, which possessed a unique electronic structure and coordination environment. This design altered the adsorption/desorption energy of reactants and intermediates, optimizing the activation pathway and enhancing electrochemical sensing performance. Under neutral conditions, the glucose sensing chip based on $PtNi_{(1:3)}$ aerogels was endowed with high sensitivity, excellent selectivity, flexibility, and outstanding long-term stability over 2 months (Fig. 7b1). To enable real-time glucose monitoring, a wearable biosensing and monitoring platform was developed, integrating a signal processing circuit and a microprogramming control unit (Fig. 7b2). This wearable sensor successfully achieved accurate, stable, real-time and non-invasive glucose monitoring in sweat on human skin.

Sweat contains other metabolites, such as UA and AA, which serve as reliable indicators for disease diagnosis and health management. Chen *et al.* prepared N-rGO/Au dual aerogels, derived from the 3D assembly of Au NPs and N-doped reduced graphene (N-rGO), to create a non-enzymatic wearable UA sensor for real-time monitoring of the UA level in sweat (Fig. 8a).[86] The synergistic combination of N-rGO and Au aerogels demonstrated superior electrocatalytic activities compared to individual components, characterized by abundant active sites, enhanced mass transfer, and improved electron transfer, as confirmed through experimental results and density functional theory (DFT) simulations. Integrated with wireless circuits, the wearable sensor enabled real-time UA monitoring, with results consistent with high performance liquid chromatography (HPLC) analysis. Furthermore, the advanced energy supply for the wearable biosensor was demonstrated by the same group, where a MA-based wearable biofuel cell (w-BFC) was developed utilizing Au/N-rGO dual aerogels and PtCu aerogels as anodic and cathodic electrocatalysts, respectively.[87] When applied to human skin, the integrated w-BFC employed an ultralow concentration of AA from sweat as a fuel to power the biosensor, facilitating real-time AA monitoring *via* a smart terminal. This approach, through the rational design of efficient electrocatalysts, can be extended to self-powered detection of other biomarkers, offering a versatile and practical solution for future wearable electronics and health management.

In clinical pathology, apart from organic compounds, hydrogen ions play a crucial role in maintaining pH balance in body fluids as well.[88] By exploiting the structural advantages of aerogels, tungsten oxide aerogels not only inherited the high chemical and mechanical stability, but also showed excellent performance in pH sensing monitoring. Wang *et al.* reported a hydrothermally synthesized tungsten oxide aerogel (TOA) as a sensing material to construct a sensitive and stable wearable pH sensor, as shown in Fig. 9.[89] The TOA possessed a fluffy porous structure consisting of ultrathin nanowires with many bifurcations, which endowed the TOA with a highly flexible

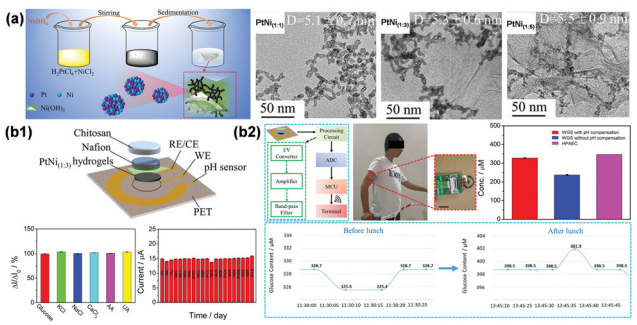

Fig. 7 (a) Synthesis, morphology and structure of the $PtNi_{(1:X)}$ dual aerogels. (b1) Schematic illustration, the selectivity and the long-term stability of the $PtNi_{(1:3)}$ aerogel-based sensing chip. (b2) Wearable application of the $PtNi_{(1:3)}$ dual aerogel-based glucose sensor (copyright 2023, John Wiley and Sons).[85]

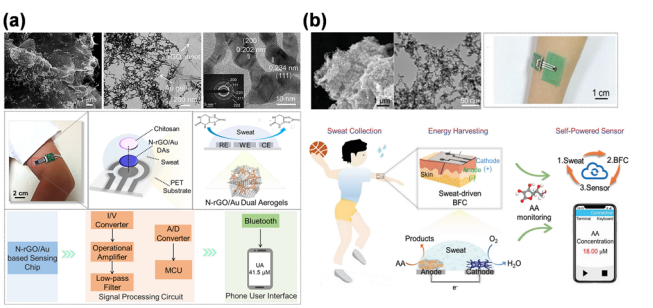

Fig. 8 (a) Nonenzymatic sweat wearable UA sensor based on N-doped reduced graphene oxide/Au dual aerogels (copyright 2024, John Wiley and Sons).[86] (b) MA-based integrated wearable biofuel cell for self-powered epidermal sweat biomarker monitoring (copyright 2023, American Chemical Society).[87]

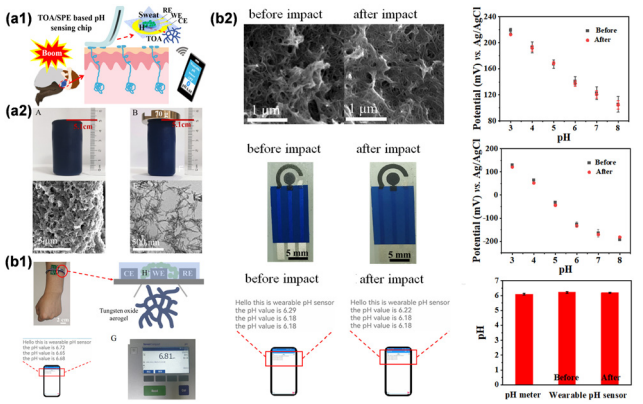

Fig. 9 Shock-resistant wearable pH sensor based on tungsten oxide aerogels (copyright 2024, Elsevier).[89]

structure with robust stability under impact environments. Combined with the signal processing circuit and Bluetooth module, the wearable pH sensor enabled non-invasive, real-time pH monitoring in sweat with minimal deviation (1.91%) compared to commercial pH meters. Additionally, the TOA-based pH wearable sensor demonstrated remarkable shock resistance, with changes limited to 7.17% under a shock of 118.38 kPa, highlighting its reliability for real-time monitoring under extreme conditions.

Conclusion and outlook

To briefly conclude, MAs hold great potential for developing wearable electrochemical biosensors, offering new possibilities for real-time health monitoring and diagnosis. Thanks to the unique properties, MAs can serve both as carriers for enzyme immobilization and as direct catalysts for biomarkers in high-performance electrochemical sensing assays. Additionally, their excellent mechanical flexibility makes them suitable for wearable applicability on elastic human skin, ensuring reliability and stability for biomarker monitoring. This review highlights recent advances in wearable electrochemical biosensors based on MAs, with our group contributing significantly to the development of wearable electrochemical sensing devices for monitoring a wide range of biomarkers, including various metabolites and ions. The functionality of MAs can be further enhanced for wearable biosensing through various strategies ranging from nanostructural design to macroscopic assembly. Despite significant advances in MA-based wearable electrochemical biosensing devices, several key challenges remain.

Firstly, issues regarding the mechanical strength and electrical conductivity of MAs have been addressed through preparation optimization, morphology adjustment of starting building blocks, and the introduction of highly conductive metals or flexible polymer hydrogels. Further development of MAs in wearable biosensing devices can focus on the following aspects: (i) enhancing biocompatibility. While MAs are typically non-toxic to cells or microorganisms, their metal ions can be toxic in certain cases. In implantable devices, the release of metal ions under specific conditions may pose a toxicity risk, limiting their application. (ii) Clarifying the multi-component synergistic effect. Interactions between different components within MAs can influence the electronic and crystal structures of the material. Understanding these mechanisms will aid in developing MAs with higher performance and expanded applications. (iii) Improving selectivity to different substrates. Unlike enzymes, which exhibit high selectivity and sensitivity, MAs are often influenced by the complexity of the microenvironment, leading to challenges in recognizing specific substrates or causing false responses. Future development in MA-based flexible electrochemical biosensors should focus on functional design strategies to broaden target monitoring, enhance flexibility and biocompatibility, and improve integration to meet practical needs for health and diagnostic management.

Data availability

No primary research results, software or code have been included and no new data were generated or analysed as part of this review.

Conflicts of interest

There are no conflicts to declare.

Acknowledgements

This work was supported by the National Natural Science Foundation of China (No. 22374119), the Key Project of Natural Science Fund of Shaanxi Province (No. 2023-JC-ZD-06 and 2024JC-YBQN-0636), and the Open Project of the State Key Laboratory of Transducer Technology (No. SKT2307).

Notes and references

1 T. Lin, Y. Xu, A. Zhao, W. He and F. Xiao, *Anal. Chim. Acta*, 2022, **1207**, 339461.
2 A. N. Vaneev, P. V. Gorelkin, A. S. Garanina, H. V. Lopatukhina, S. S. Vodopyanov, A. V. Alova, O. O. Ryabaya, R. A. Akasov, Y. Zhang, P. Novak, S. V. Salikhov, M. A. Abakumov, Y. Takahashi, C. R. W. Edwards, N. L. Klyachko, A. G. Majouga, Y. E. Korchev and A. S. Erofeev, *Anal. Chem.*, 2020, **92**, 8010–8014.
3 Y. Yu, H. Y. Y. Nyein, W. Gao and A. Javey, *Adv. Mater.*, 2020, **32**, 1902083.
4 M. S. Sumitha and T. S. Xavier, *Hybrid Adv.*, 2023, **2**, 100023.
5 M. Wei, Y. Qiao, H. Zhao, J. Liang, T. Li, Y. Luo, S. Lu, X. Shi, W. Lu and X. Sun, *Chem. Commun.*, 2020, **56**, 14553–14569.
6 J. Wu, H. Liu, W. Chen, B. Ma and H. Ju, *Nat. Rev. Bioeng.*, 2023, **1**, 346–360.
7 A. Das, X. Cui, V. Chivukula and S. S. Iyer, *Anal. Chem.*, 2018, **90**, 11589–11598.
8 L. C. Clark and C. Lyons, *Ann. N. Y. Acad. Sci.*, 1962, **102**, 29–45.
9 K. Nemčeková and J. Labuda, *Mater. Sci. Eng., C*, 2021, **120**, 111751.
10 N. Thakur, D. Gupta, D. Mandal and T. C. Nagaiah, *Chem. Commun.*, 2021, **57**, 13084–13113.
11 W. He, B. Qiao, F. Li, L. Pan, D. Chen, Y. Cao, J. Tu, X. Wang, C. Lv and Q. Wu, *Chem. Commun.*, 2021, **57**, 619–622.
12 M. Labib, E. H. Sargent and S. O. Kelley, *Chem. Rev.*, 2016, **116**, 9001–9090.
13 F. Mazzara, B. Patella, G. Aiello, A. O'Riordan, C. Torino, A. Vilasi and R. Inguanta, *Electrochim. Acta*, 2021, **388**, 138652.

14 J. F. Hernández-Rodríguez, D. Rojas and A. Escarpa, *Anal. Chem.*, 2021, **93**, 167–183.
15 M. D. Steinberg, P. Kassal and I. M. Steinberg, *Electroanalysis*, 2016, **28**, 1149–1169.
16 J. Park, J. Kim, S.-Y. Kim, W. H. Cheong, J. Jang, Y. G. Park, K. Na, Y. T. Kim, J. H. Heo, C. Y. Lee, J. H. Lee, F. Bien and J. U. Park, *Sci. Adv.*, 2018, **4**, eaap9841.
17 M. Bariya, H. Y. Y. Nyein and A. Javey, *Nat. Electron.*, 2018, **1**, 160–171.
18 J. Kim, A. S. Campbell, B. E.-F. de Ávila and J. Wang, *Nat. Biotechnol.*, 2019, **37**, 389–406.
19 Y. Gao, L. Yu, J. C. Yeo and C. T. Lim, *Adv. Mater.*, 2020, **32**, 1902133.
20 K. Takei, T. Takahashi, J. C. Ho, H. Ko, A. G. Gillies, P. W. Leu, R. S. Fearing and A. Javey, *Nat. Mater.*, 2010, **9**, 821–826.
21 B. An, Y. Ma, W. Li, M. Su, F. Li and Y. Song, *Chem. Commun.*, 2016, **52**, 10948–10951.
22 J. Ma, Y. Jiang, L. Shen, H. Ma, T. Sun, F. Lv, A. Kiran and N. Zhu, *Biosens. Bioelectron.*, 2019, **144**, 111637.
23 L. Zheng, M. Zhu, B. Wu, Z. Li, S. Sun and P. Wu, *Sci. Adv.*, 2021, **7**, eabg4041.
24 L. Wang, X. He, Y. Hao, M. Zheng, R. Wang, J. Yu and X. Qin, *Sci. China Mater.*, 2023, **66**, 707–715.
25 C. Lim, Y. Shin, J. Jung, J. H. Kim, S. Lee and D. H. Kim, *APL Mater.*, 2018, **7**, 31502.
26 R. Du, J.-O. Joswig, R. Hübner, L. Zhou, W. Wei, Y. Hu and A. Eychmüller, *Angew. Chem.*, 2020, **132**, 8370–8377.
27 A. A. Dubale, Y. Zheng, H. Wang, R. Hübner, Y. Li, J. Yang, J. Zhang, N. K. Sethi, L. He, Z. Zheng and W. Liu, *Angew. Chem., Int. Ed.*, 2020, **59**, 13891–13899.
28 H. Zhang, W. Han, K. Xu, Y. Zhang, Y. Lu, Z. Nie, Y. Du, J. Zhu and W. Huang, *Nano Lett.*, 2020, **20**, 3449–3458.
29 S. Yan, M. Zhong, C. Wang and X. Lu, *Chem. Eng. J.*, 2022, **430**, 132955.
30 G. W. Qin, J. Liu, T. Balaji, X. Xu, H. Matsunaga, Y. Hakuta, L. Zuo and P. Raveendran, *J. Phys. Chem. C*, 2008, **112**, 10352–10358.
31 N. C. Bigall, A. K. Herrmann, M. Vogel, M. Rose, P. Simon, W. Carrillo-Cabrera, D. Dorfs, S. Kaskel, N. Gaponik and A. Eychmüller, *Angew. Chem., Int. Ed.*, 2009, **48**, 9731–9734.
32 R. Du, W. Jin, H. Wu, R. Hübner, L. Zhou, G. Xue, Y. Hu and A. Eychmüller, *J. Mater. Chem. A*, 2021, **9**, 17189–17197.
33 M. Oezaslan, W. Liu, M. Nachtegaal, A. I. Frenkel, B. Rutkowski, M. Werheid, A.-K. Herrmann, C. Laugier-Bonnaud, H. C. Yilmaz, N. Gaponik, A. Czyrska-Filemonowicz, A. Eychmüller and T. J. Schmidt, *Phys. Chem. Chem. Phys.*, 2016, **18**, 20640–20650.
34 L. Nahar, A. A. Farghaly, R. J. A. Esteves and I. U. Arachchige, *Chem. Mater.*, 2017, **29**, 7704–7715.
35 Q. Shi, C. Zhu, H. Zhong, D. Su, N. Li, M. H. Engelhard, H. Xia, Q. Zhang, S. Feng, S. P. Beckman, D. Du and Y. Lin, *ACS Energy Lett.*, 2018, **3**, 2038–2044.
36 S. M. Jung, H. Y. Jung, M. S. Dresselhaus, Y. J. Jung and J. Kong, *Sci. Rep.*, 2012, **2**, 849.
37 F. J. Burpo, E. A. Nagelli, L. A. Morris, J. P. McClure, M. Y. Ryu and J. L. Palmer, *J. Mater. Res.*, 2017, **32**, 4153–4165.
38 B. Cai, V. Sayevich, N. Gaponik and A. Eychmüller, *Adv. Mater.*, 2018, **30**, 1707518.
39 N. Leventis, N. Chandrasekaran, C. Sotiriou-Leventis and A. Mumtaz, *J. Mater. Chem.*, 2009, **19**, 63–65.
40 N. Leventis, N. Chandrasekaran, A. G. Sadekar, S. Mulik and C. Sotiriou-Leventis, *J. Mater. Chem.*, 2010, **20**, 7456–7471.
41 D. Wen, W. Liu, D. Haubold, C. Zhu, M. Oschatz, M. Holzschuh, A. Wolf, F. Simon, S. Kaskel and A. Eychmüller, *ACS Nano*, 2016, **10**, 2559–2567.
42 W. Duan, P. Zhang, Y. Xiahou, Y. Song, C. Bi, J. Zhan, W. Du, L. Huang, H. Möhwald and H. Xia, *ACS Appl. Mater. Interfaces*, 2018, **10**, 23081–23093.
43 S. Naskar, A. Freytag, J. Deutsch, N. Wendt, P. Behrens, A. Köckritz and N. C. Bigall, *Chem. Mater.*, 2017, **29**, 9208–9217.
44 X. Jiang, R. Du, R. Hübner, Y. Hu and A. Eychmüller, *Matter*, 2021, **4**, 54–94.
45 W. Liu, A. Herrmann, D. Geiger, L. Borchardt, F. Simon, S. Kaskel, N. Gaponik and A. Eychmüller, *Angew. Chem., Int. Ed.*, 2012, **51**, 5743–5747.
46 Y. Jin, F. Chen, J. Wang, L. Guo, T. Jin and H. Liu, *J. Power Sources*, 2019, **435**, 226798.
47 B. Jiang, Z. Wan, Y. Kang, Y. Guo, J. Henzie, J. Na, H. Li, S. Wang, Y. Bando, Y. Sakka and Y. Yamauchi, *Nano Energy*, 2021, **81**, 105644.
48 Q. Fang, Y. Qin, H. Wang, W. Xu, H. Yan, L. Jiao, X. Wei, J. Li, X. Luo, M. Liu, L. Hu, W. Gu and C. Zhu, *Anal. Chem.*, 2022, **94**, 11030–11037.
49 B. Cai, D. Wen, W. Liu, A. K. Herrmann, A. Benad and A. Eychmüller, *Angew. Chem., Int. Ed.*, 2015, **54**, 13101–13105.
50 H. Yuan, X. Wan, J. Ye, T. Ma, F. Ma, J. Gao, W. Gao and D. Wen, *Adv. Funct. Mater.*, 2023, **33**, 2302561.
51 W. Pan, C. Liang, Y. Sui, J. Wang, P. Liu, P. Zou, Z. Guo, F. Wang, X. Ren and C. Yang, *Adv. Funct. Mater.*, 2022, **32**, 2204166.
52 X. Xu, R. Wang, P. Nie, Y. Cheng, X. Lu, L. Shi and J. Sun, *ACS Appl. Mater. Interfaces*, 2017, **9**, 14273–14280.
53 Y. Tang, S. Gong, Y. Chen, L. W. Yap and W. Cheng, *ACS Nano*, 2014, **8**, 5707–5714.
54 S. M. Jung, H. Y. Jung, M. S. Dresselhaus, Y. J. Jung and J. Kong, *Sci. Rep.*, 2012, **2**, 849.
55 F. Qian, P. C. Lan, M. C. Freyman, W. Chen, T. Kou, T. Y. Olson, C. Zhu, M. A. Worsley, E. B. Duoss, C. M. Spadaccini, T. Baumann and T. Y. J. Han, *Nano Lett.*, 2017, **17**, 7171–7176.
56 F. Lübkemann, J. F. Miethe, F. Steinbach, P. Rusch, A. Schlosser, D. Zámbó, T. Heinemeyer, D. Natke, D. Zok, D. Dorfs and N. C. Bigall, *Small*, 2019, **15**, 1902186.
57 N. Gaponik, A. K. Herrmann and A. Eychmüller, *J. Phys. Chem. Lett.*, 2012, **3**, 8–17.
58 X. Tong, L. Ga, L. Bi and J. Ai, *Electroanalysis*, 2023, **35**, e202200228.
59 S. Carreiro, K. Wittbold, P. Indic, H. Fang, J. Zhang and E. W. Boyer, *J. Med. Toxicol.*, 2016, **12**, 255–262.
60 F. Sassa, G. Chandra Biswas and H. Suzuki, *Lab Chip*, 2020, **20**, 1358–1389.
61 C. Dincer, R. Bruch, E. Costa-Rama, M. T. Fernández-Abedul, A. Merkoçi, A. Manz, G. A. Urban and F. Güder, *Adv. Mater.*, 2019, **31**, 1806739.
62 Q. Huang and Y. Zhu, *Adv. Mater. Technol.*, 2019, **4**, 1970029.
63 S. Hales, E. Tokita, R. Neupane, U. Ghosh, B. Elder, D. Wirthlin and Y. L. Kong, *Nanotechnology*, 2020, **31**, 172001.
64 W. Gao and D. Wen, *View*, 2021, **2**, 20200124.
65 Q. Sun, M. Xu, S. J. Bao and C. M. Li, *Nanotechnology*, 2015, **26**, 115602.
66 J. M. Jeong, M. Yang, D. S. Kim, T. J. Lee, B. G. Choi and D. H. Kim, *J. Colloid Interface Sci.*, 2017, **506**, 379–385.
67 C. I. Fort, R. Ortiz, L. C. Cotet, V. Danciu, I. C. Popescu and L. Gorton, *Electroanalysis*, 2016, **28**, 2311–2319.
68 D. Wen, A. K. Herrmann, L. Borchardt, F. Simon, W. Liu, S. Kaskel and A. Eychmüller, *J. Am. Chem. Soc.*, 2014, **136**, 2727–2730.
69 C. D. Ruiz-Guerrero, D. V. Estrada-Osorio, A. Gutiérrez, F. I. Espinosa-Lagunes, R. A. Escalona-Villalpando, G. Luna-Bárcenas, A. Molina, A. Arenillas, L. G. Arriaga and J. Ledesma-García, *Biosens. Bioelectron.*, 2025, **267**, 116850.
70 D. Wen, W. Liu, D. Haubold, C. Zhu, M. Oschatz, M. Holzschuh, A. Wolf, F. Simon, S. Kaskel and A. Eychmüller, *ACS Nano*, 2016, **10**, 2559–2567.
71 Y. Yang, H. Zhang, J. Wang, S. Yang, T. Liu, K. Tao and H. Chang, *J. Mater. Chem. A*, 2019, **7**, 11497–11505.
72 Q. Fang, H. Wang, X. Wei, Y. Tang, X. Luo, W. Xu, L. Hu, W. Gu and C. Zhu, *Adv. Healthcare Mater.*, 2023, **12**, 2301073.
73 R. G. Mahmudunnabi, F. Z. Farhana, N. Kashaninejad, S. H. Firoz, Y.-B. Shim and M. J. A. Shiddiky, *Analyst*, 2020, **145**, 4398–4420.
74 G. Li, Y. Chen, F. Liu, W. Bi, C. Wang, D. Lu and D. Wen, *Microsyst. Nanoeng.*, 2023, **9**, 152.
75 G. Li, P. Xue, H. Fan, Y. Ma, H. Wang, D. Lu, J. Gao and D. Wen, *Anal. Chim. Acta*, 2024, **1306**, 342613.
76 K. Mahato and J. Wang, *Sens. Actuators, B*, 2021, **344**, 130178.
77 Y. Cao, H. Shi, C. Yi, Y. Zheng, Z. Tan, X. Jia and Z. Liu, *TrAC, Trends Anal. Chem.*, 2024, **172**, 117561.
78 T. Wu, X. You and Z. Chen, *Sensors*, 2022, **22**, 4253.
79 C. Chen, Y. Fu, S. S. Sparks, Z. Lyu, A. Pradhan, S. Ding, N. Boddeti, Y. Liu, Y. Lin, D. Du and K. Qiu, *ACS Sens.*, 2024, **9**, 3212–3223.
80 S. Naveena and A. Bharathi, *Biomed. Signal Process. Control*, 2022, **77**, 103748.
81 A. R. Nasser, A. M. Hasan, A. J. Humaidi, A. Alkhayyat, L. Alzubaidi, M. A. Fadhel, J. Santamaría and Y. Duan, *Electronics*, 2021, **10**, 2719.
82 M. D. Steinberg, P. Kassal and I. M. Steinberg, *Electroanalysis*, 2016, **28**, 1149–1169.
83 Ö. Kap, V. Kılıç, J. G. Hardy and N. Horzum, *Analyst*, 2021, **146**, 2784–2806.

84 G. Li, J. Hao, W. Li, F. Ma, T. Ma, W. Gao, Y. Yu and D. Wen, *Anal. Chem.*, 2021, **93**, 14068–14075.
85 G. Li, C. Wang, Y. Chen, F. Liu, H. Fan, B. Yao, J. Hao, Y. Yu and D. Wen, *Small*, 2023, **19**, 2206868.
86 Y. Chen, G. Li, W. Mu, X. Wan, D. Lu, J. Gao and D. Wen, *Anal. Chem.*, 2023, **95**, 3864–3872.
87 Y. Chen, X. Wan, G. Li, J. Ye, J. Gao and D. Wen, *Adv. Funct. Mater.*, 2024, 2404329.
88 Y. Lei, W. Zhao, Y. Zhang, Q. Jiang, J. H. He, A. J. Baeumner, O. S. Wolfbeis, Z. L. Wang, K. N. Salama and H. N. Alshareef, *Small*, 2019, **15**, 1901190.
89 C. X. Wang, G. L. Li, Y. Hang, D. F. Lu, J. Q. Ye, H. Su, B. Hou, T. Suo and D. Wen, *Chin. Chem. Lett.*, 2024, 110502.